Memoirs of the Faculty of Engineering, Nagoya University
Vol. 33, No. 2 (1981)

VERIFICATION OF SIMILARITY THEORY ON SPACE AIR DISTRIBUTION AND STUDY ON OCCUPIED ZONE AIR-CONDITIONING FOR LARGE SPACES THROUGH SCALED MODEL EXPERIMENTS AND ACTUAL MEASUREMENTS

NOBUO NAKAHARA

Department of Architecture

(Received October 17, 1981)

Abstract

It is considered desirable that air-conditioning for large spaces should be restricted only to the space within the occupied zone from the viewpoint of economical feasibility and energy conservation.

This is a report on the application of the occupied zone air-conditioning to three different large spaces: an exposition hall, a sport hall and a factory of large machine assembly at constant temperature. The distribution of air and temperature were first examined by the experiments with the scaled models followed by the actual measurements. The results obtained by the experiments have proved that the proposed similarity theory on space air distribution can be verified after comparing them with the predicted values. The heat load calculation method for the occupied zone air-conditioning is also proposed in this paper. In addition, the performance of the induction type of outlets suitable for large spaces are analyzed by experiments in detail.

CONTENTS

1. Forward

In the case of air-conditioning of a large space, it is considered desirable to restrict the conditioned space only to the so-called occupied zone by securing proper distribution of air and temperature within that zone with regard to economical feasibility and energy conservation.

Very few reports on what we call the occupied zone air-conditioning can be

found. On the other hand, the similarity theory on space air distribution with the model and actual experiments can not be said as fully verified.

For these purposes, at the stage of planning, it is necessary to study and predict the distribution characteristics of air and temperature for various types and locations of outlets and inlets, outlet velocity and ventilation rate. In addition, the possible amounts of monetary and energy savings as compared with the conventional systems should be estimated beforehand.

Although the numerical simulation which solves the fundamental equations of fluid is recently being attempted, it stands far from practical use, especially when the configurations and locations of outlets and inlets are complicated. Therefore the experiments with scaled models have been admitted as the most practical and more precise as the technique for simulating an air distribution. While in practice the heat load calculation for such air-conditioning excluding the upper part of the large space, simplifying techniques must be prepared for taking account of the heat exchange caused by natural or forced ventilation between upper and lower parts, radiation from the heated walls, roofs, lights, and miscellaneous objects located in the upper zone.

For the purpose of developing these techniques, verification of the similarity theory applicable to the model tests in comparison with the actual measurements is considered the most essential. The object of the present study can be summarized as follows.

1) To plan the occupied zone air-conditioning system with the most appropriate air distribution scheme matching to the conditions in accordance with the application of the large scale space.

2) To predict the distribution of air and temperature in the actual structure with the scaled model tests and to determine the detailed conditions of the optimum outlets and inlets which can be matched with the design conditions of the space.

3) To verify the similarity theory applied to tests by comparing with the actual measurements after completion.

4) To investigate and establish the heat load calculation methodology for the occupied zone air-conditioning system, and to make it possible to predict the amount of monetary and energy savings.

Large scale spaces selected for the said purposes are Midori Kan (Pavilion) Exposition Hall utilized for hemispherical film projection, Kuramae-Kokugikan (Sumo Arena) and M-factory for assembly of large and precise machines which needs a constant room air temperature.

Verification of the similarity theory and analysis on the characteristics of the induction type of outlets were the main subjects in the first example. The second example was set to study the optimum air distribution system in the occupied zone air-conditioning of such kinds of building as sports arena backed up by the results obtained in the first example. In the third example, proposal and verification of the heat load calculation method for the occupied zone air-conditioning system are added to the purposes with the above two examples.

2. Air-Conditioning for Large Spaces

2. 1. The Occupied Zone Air-Conditioning

The space in large spaces occupied by persons or industrial products are generally restiricted to the lower zone within a few meters above the floor. Therefore, at the designing of air-conditioning systems for them, the space which requires an air-conditioning can be restricted only to the lower occupied zone leaving the upper zone unconsidered. When the conditioned space can be confined only to the space around the seats as in the case of theater, the seat air-conditioning system is occasionally adopted, in which numerous numbers of air outlets are provided just under the seats.

In many cases, however, wall-mounted nozzle type of outlets having a long throw distance are generally employed in order to secure flexible use of the floor area. It is desirable that the discharge angle of air outlets can be adjusted freely to meet with different kinds of conditions, i. e., cooling, heating, heating before occupancy and isothermal conditions. In order to prevent the stagnation of air flow near the outlets, the induction type of air outlets may be employed.

The radiant panel heating is often recommended as one of the most desirable occupied zone heating for a large space. In a theater or sport arena, however, the ventilation to eliminate smoke and dust generated in the room is required: this may be achieved by the central air distribution system in combination with the panel heating system, but causes high initial and running costs. For this reason, when heating is required in the following projects, only warm air heating system is adopted principally.

2. 2. Pattern of Systems

Fig. 1 shows various air-conditioning systems for large spaces. As shown in Fig. 1(a) and (b), it is supposed as most desirable to induce a secondary air circuit to remove the heat, dust and smoke which stagnate in the unconditioned upper zone.

Fig. 1(a) shows the system in which the air to be exhausted for ventilation is reused for the secondary air circuit in the upper zone befre being exhausted to outside. Since the air volume to be blown out into the upper zone is equal to the air volume to be discharged from the ceiling, the air mixing between the lower conditioned space and the upper unconditioned space can be kept to the minimum. Since the temperature of the air blown into the upper zone is almost equal to that of the ocuupied zone, cooling or heating effect upon the inner surfaces of the ceiling as well as the upper part of the wall surface can be expected to some extent.

Fig. 1(b) shows the system in which outside air is utilized for the ventilation of the upper zone. To prevent the down-draft effect and the cooling of the surfaces in the upper zone by cold outside air, operation with this circuit must be closed in winter. Therefore, this type is not suitable for such buildings as theaters, sports arenas and factories which require exhaust systems through the ceiling to remove smoke and dust from the space.

Fig. 1(c) might be one of the most economical system in terms of initial cost. However, considerable differences in temperature between the upper zone and the

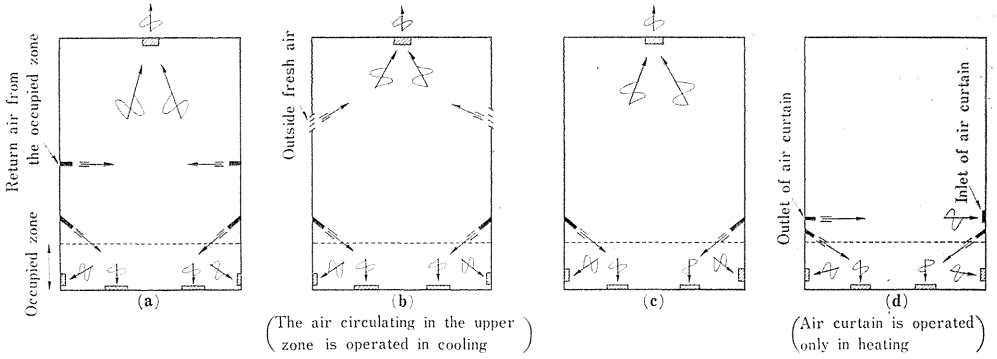

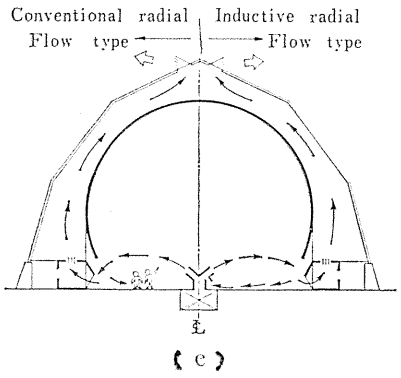

Fig. 1. Air-conditioning systems for larger spaces.

occupied zone will be generated in heating, as part of the air blown into the occupied zone is to be drawn to the upper zone.

Fig. 1(d) shows the system which employs an air curtain to prevent the uprise of warm air in the case of heating.

Fig. 1(e) shows a special example in which the air outlets can be provided on the floor of the occupied zone. By adopting the radial flow outlets, the occupied zone air conditioning can be simply performed. In addition, the exhaust air that flows through the cavity behind the ceiling removes the heat from the roof. In this way, the system applied to the occupied zone air-conditioning must be carefully evaluated for the selection in consideration with the usage of the large space, the design conditions and the importance of ventilation. As shown in the following chapter, all three examples discribed in this article have adopted different systems for the same purpose to establish occupied zone air-conditioning.

3. Model Experiments for Air Distribution in a Room

3. 1. Similarity Theory of Room Air Distribution under Non-isothermal Conditions

Room air under the conditions of forced ventilation may be considered as being in a completely turbulent region with the exception of an extremely thin zone

at the boundary layer. It was reported that the coefficient of vortex viscosity which gives great influence upon the turbulent air flow in a room has been obtained from a series of experiments as being proportional to the scale of the room as follows:

$$\kappa \propto v \cdot l \tag{1}$$

where

κ: coefficient of vortex viscosity (m^2/s)

v: air velocity (m/s)

l: characteristic linear dimension (m)

For the similarity of room air distribution within a turbulent flow region, it is necessary to equate the following dimensionless numbers both the model and actual, which can be obtained by reducing the basic equations of fluids to dimensionless form.

turbulent Reynolds number

$$Re = \frac{vl}{\kappa} \tag{2}$$

turbulent Peclet number

$$Pe = Re \cdot Pr = \frac{vl}{\kappa} \cdot \frac{\kappa}{a} = \frac{v \cdot l}{a} \tag{3}$$

Archimedes number

$$Ar = \frac{Gr}{Re^2} = \frac{g \cdot \beta \cdot \Delta t \cdot l}{v^2} \tag{4}$$

where

a: coefficient of vortex thermal diffusivity (m^2/s)

g: gravitational acceleration constant (m/s^2)

β: coefficient of volumetric expansion ($=1/273+t$), (1/deg)

Δt: temperature difference between two points in a room (deg)

Re: Reynolds number

Pr: Prandtl number

Gr: Grashof number

From Eq. (1), the turbulent Reynolds number may be assumed to have constant value regardless of the model size. Meanwhile, in the case of normal experiments using air, Prandtl number may similarly be assumed to have a constant value. From this fact the turbulent Peclet number can be assumed to be constant. Accordingly, the room air distribution will be similar if only a common value of Archimedes number were selected for both. In short, if only the air velocity at the outlet and the temperature difference between the outlet and the certain representative point in the occupied zone are taken as the characteristic values of air velocity and temperature difference respectively and if the Archimedes number between the model and the actual is matched, then the pattern of air flow within

the room comes out as almost similar.

Suppose now that the reduction ratio of the model to the actual is n, the following relationship may be established among the reduction ratio of linear dimension (n_l), reduction ratio of temperature difference between air outlet and occupied zone ($n_{\Delta t}$), and reduction ratio of air velocity at the outlet (n_{v_0}):

$$n_{\Delta t} \cdot n_l / n_{v_0}^2 = 1 \tag{5}$$

where

v_0: Air velocity at the outlet (m/s)

Further, suppose that the reduction ratio of inside heat generation is n_Q, the following equation can be derived from the equation of heat balance at the boundary surfaces around the inside heat generating body:

$$n_{v_0} \cdot n_l^2 \cdot n_{\Delta t} / n_Q = 1 \tag{6}$$

It is possible to estimate the actual air distribution from the results of model experiment by multiplying $1/n_{v_0}$ in terms of velocity and $1/n_{\Delta t}$ in terms of temperature, taking air temperature at the outlet for the reference.

Taking the reduction ratio of linear dimension n and temperature difference $n_{\Delta t}$ for the reference, the variables of the model can be expressed as follows:

for air velocity,

$$v_M = \left(\frac{1}{v_N}\right) \cdot \left(\frac{1}{n}\right)^{\frac{1}{2}} \cdot \left(\frac{1}{n_{\Delta t}}\right)^{\frac{1}{2}} \tag{7}$$

for air volume

$$V_M = \left(\frac{1}{V_N}\right) \cdot \left(\frac{1}{n}\right)^{\frac{5}{2}} \cdot \left(\frac{1}{n_{\Delta t}}\right)^{\frac{1}{2}} \tag{8}$$

for heat generation

$$Q_M = \left(\frac{1}{Q_N}\right) \cdot \left(\frac{1}{n}\right)^{\frac{5}{2}} \cdot \left(\frac{1}{n_{\Delta t}}\right)^{\frac{3}{2}} \tag{9}$$

In the equations suffix M indicates the model and suffix N the actual. In the experiment, outlet air temperature of the model may be selected freely, and then heating and cooling rate supplied from outside of the model for cooling and heating respectively should be controlled so as to obtain the temperature difference (Δt) as predetermined from Eq. (5). In this method, the similarity of heat resistance of the composite walls between the model and the actual is not necessarily taken into account. Beside this, there is another method of experiment which takes the outside air temperature for the reference. Allowing for the exact estimation of heat load of the building as well as air distribution, this method is not considered practical for the difficulty in realizing such similarity conditions simultaneously in terms of heat resistances of composite walls, coefficient of heat transfer along wall surfaces and radiation exchange between enclosure surfaces.

The scale factors employed in the three model experiments described in the following chapter are shown in Table 1.

Table 1. Various scale factors of three model experiments.

		Midori Pavilion	Kuramae Kokugikan	M- Factory
n_l		0.1(1/10)	0.0833(1/12)	0.1(1/10)
$n_{\Delta t}$	for cooling	1.65	3.0	1.0
	for heating		2.0	1.0
n_v	for cooling	0.406	0.500	0.316
	for heating		0.408	0.316

3. 2. Room and Air-Conditioning Apparatus for Model Experiments

Model experiments were performed in the air-conditioning test room of Ohbayashigumi Technical Research Institute. Fig. 2 shows the diagram of the apparatus for model experiments. Chilled water and hot water are stored in the underground heat storage tank during the experiments.

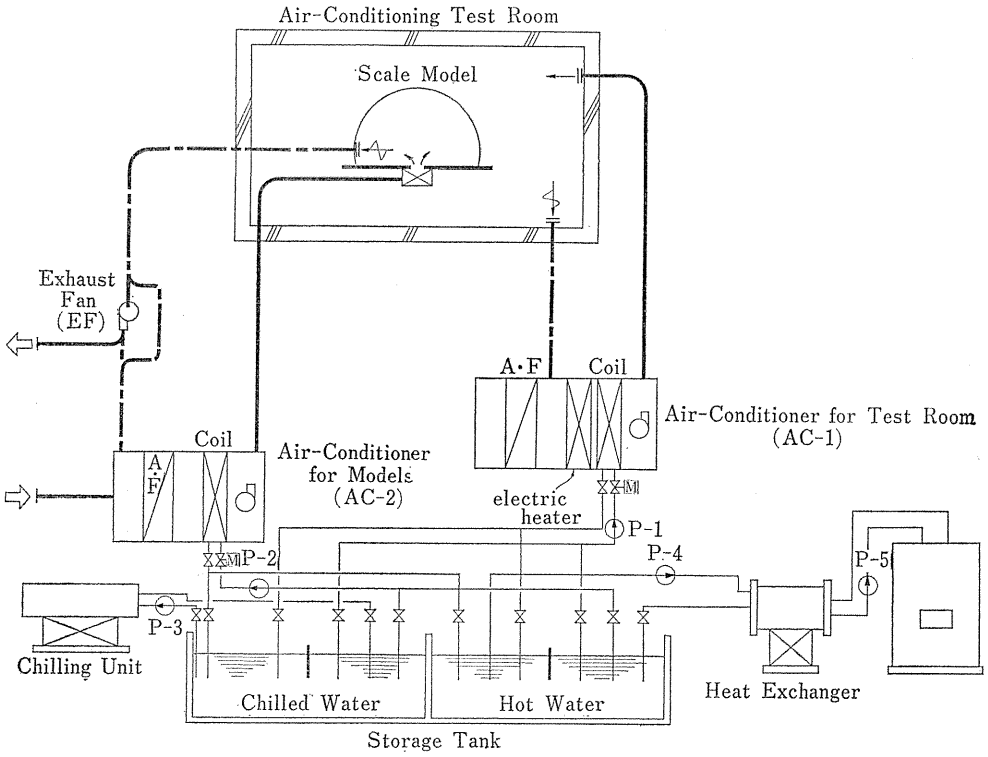

Fig. 2. Simplified system diagram of air-conditioning apparatus for model experiments.

AC-1 is provided for conditioning the air around the model and it has heating

as well as cooling elements controlled automatically. AC-2 supplies the air to the model, the air condition of which is determined by the similarity theory for the model. Air quantity is measured by using Pitot tube. Heat storage tank gives the good flexibility for producing heat supply in any form.

4. The Case of Midori Pavilion

In the basic scheme of the air-conditioning plan for the Midori Pavilion at Expo. '70, considerations were given so that the conditioned air supply system could satisfy the following items:

(a) No hindrance to projection functions of the hemispheric-vision film projection "Astrorama".

(b) Supply system taking full advantage of the characteristics of a domed space.

(c) Economization of air-conditioning installations.

(d) Securing of uniform air distribution in occupied zone.

As the results, it was considered that the most ideal system would be obtained by providing a single, large-sized outlet at the center of the circular floor. However, there were not many past cases of air-conditioning of large spaces with a large single outlet especially with unique air flow pattern, and there were utterly no deta on air distribution in such cases. Therefore, the general characteristics of special large-sized outlets such as centerline velocity constants, velocity profiles of jets, inductive performance and static pressure losses were first obtained through experiments for the study. Space air distribution inside the dome was next sought through experiments with scale models and the most appropriate supply outlet shape was determinded. Further, actual measurements were made under the same conditions as those employed in the scale model experiments and the accuracy of the similarity theory of models was pursued through comparison with estimated values obtained in the model experiments.

4. 1. Outline of Building

4. 1. 1. Outline of Architecture

The Midori Pavilion, which was completed at the end of 1969 for Expo. '70, and dismantled after the fair, was a hemispherical building of unique design with steel beams assembled in triangular shape and with fiber-reinforced plastic panels used as exterior surfacing. The height above ground level was 27.6 m and the building area was 3,047 m^2. A hemisphere-shaped screen was provided on the interior side of the dome and a film image called "Astrorama" was projected on the entire ceiling and sides using 5 projectors. The exterior view of the building is shown in Fig. 3. The plan of the pavilion is shown in Fig. 4.

4. 1. 2. Outline of Air-Conditioning System

District chilled water supplied by the Expo Association was sent as the heat sink to air handling apparatus employing a secondary circulating pump. Conditioned air blown into the dome entered the projection rooms through return inlets at the sides of the dome to remove heat generated by the projectors, and in order also

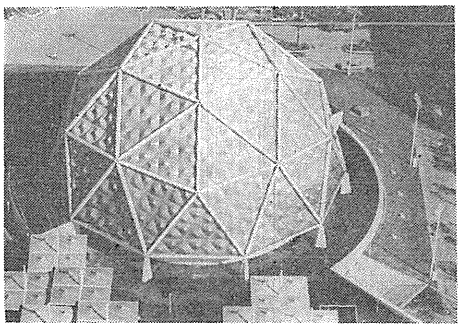

Fig. 3. Exterior view of the Midori Pavilion.

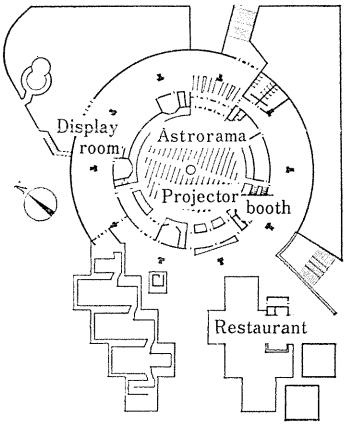

Fig. 4. Plan of the Midori Pavilion.

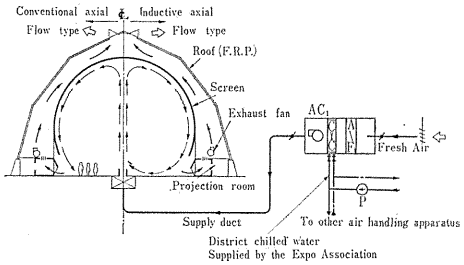

Fig. 5. Air flow patterns by conventional and inductive axial flow (nozzle type) outlets.

to remove loads entering from the roof, the air was exhausted outside through the space between screen and roof and through louvers at the top. To increase the purity of air, adequate air filters were provided and all-fresh-air air-conditioning was carried out. The cooling load within the dome was approximately 170, 000kcal/h, total cooling capacity of apparatus approximately 400, 000 kcal/h and supply air

Table 2. Data on heat load and ventilation of the air-conditioning system for the Midori Pavilion.

Room Cooling Load	166, 400 kcal/h
S H F	54%
Outside Air Load	209, 000 kcal/h
Cooling Lood	400, 000 kcal/h
Primary Air Volume	25, 000 m^3/h
Room Load per unit floor area	243 $kcal/m^2h$
Air Volume per unit floor area	37 m^3/m^2h
Air Change	2.2/h

volume approximately 25,000m³/h. Fig. 5 shows the simplified diagram of the air-conditioning system and air flow patterns with supposed nozzle type outlets.

Table 2 shows the data on heat load and ventilation of this air-conditioning system.

4. 1. 3. Supply Air Outlet

In making the decision to provide a single large-sized supply air outlet at the center of the circular floor, four varieties of shapes were considered.

(a) *Conventional Axial Flow (Nozzle Type) Outlet*

The air flow pattern is shown at the left-hand side of Fig. 5. Conditioned air blown out from the center of the floor toward the top descends along the surface of the screen and enters the occupied zone, which may be called a "membrane cooling system." If a reasonable air velocity and diamater of outlet should be selected, the velocity of air in the vicinity of the top of the dome corresponding to the end of Zone 2 of the jets obtained from the relation between the flow length and the diamater of outlet becomes considerably high. For this reason, this system would cause the screen to vibrate due to air flow thereby adversely affecting the projection of "Astorama" and would therefore be subjected to considerable limitations for practical purposes.

(b) *Inductive Axial Flow (Nozzle Type) Outlet*

This outlet possesses an inductive function for secondary air near the outlet due to the fact that a conical secondary nozzle is additionally provided outside of conventional primary nozzle. The air flow pattern is as shown at the right-hand side of Fig. 5. Compared with a simple nozzle outlet the primary air volume is natuarally reduced if the rate of air ventilation is maintained constant, and conversely, the rate of air ventilation is increased if the primary air volume is fixed. Economy of air-conditioning apparatus as well as duct works can be attained with this system.

(c) *Conventional Radial Flow Outlet*

This outlet provides an air flow pattern in which air is blown out radially, and the form of air flow is such that the occupied zone is enveloped in an area of entrainment. With respect to the characteristics of air flow distribution, calculations can be made for Zone 3 and diffusibility is high. Moreover, a big advantage is that only the occupied zone is cooled, since the temperature of the upper part of the dome is allowed to vary arbitrarily, and the cooling load can be lessened. The air flow pattern is shown at the left-hand side of Fig. 1(e).

(d) *Inductive Radial Flow Outlet*

In this outlet there is a conical primary nozzle inside the conventional radial flow outlet described in (c), producing a secondary air flow in the vicinity of the outlet. As in the case of the outlet described in (b), there is no stagnation of air in the occupied zone near the center of the circular floor and a uniform air distribution can be expected. The characteristics of the occupied zone cooling effect and the lessened cooling load are almost the same as those in (c). The air flow pattern is indicated at the right-hand side of Fig. 1(e). Among these, axial flow (nozzle type) outlets located on the floor are not suitable for the occupied zone

air-conditioning from the viewpoint of economical feasibility and energy savings.

4. 2. Scaled Model Experiments

The reduction ratio of the scaled model is as shown in Table 1.

As stated in the preceding chapter the scale of models to be used in the experiments must be determined from the Archimedes number. The testing accuracy is improved with larger n, but the economic balance of the test costs should be taken into account. In the present experiment there were restrictions with respect to the size of the testing room and precisions of measuring instruments, particularly the anemometer. It was found that, with $n_{\Delta t}=1.65$ and $n_v=0.406$, the scale of the model would be one-tenth, which was suitable for these experiments. Fig. 6 shows experimentally-made air outlets employed in the model tests to find the characteristics of single air outlets. In each of the types the left-hand side shows a cross section and the right-hand side an elevation. Further, the discharge angles (θ) and heights (H) in Type P-1 and Type P-2 are freely adjustable. Experiments are classified into two parts. One is the isothermal experiments to identify the general characteristics of these peculiar large scale outlets, and the other is non-isothermal experiments to search for the optimum outlet type as well as room air distribution.

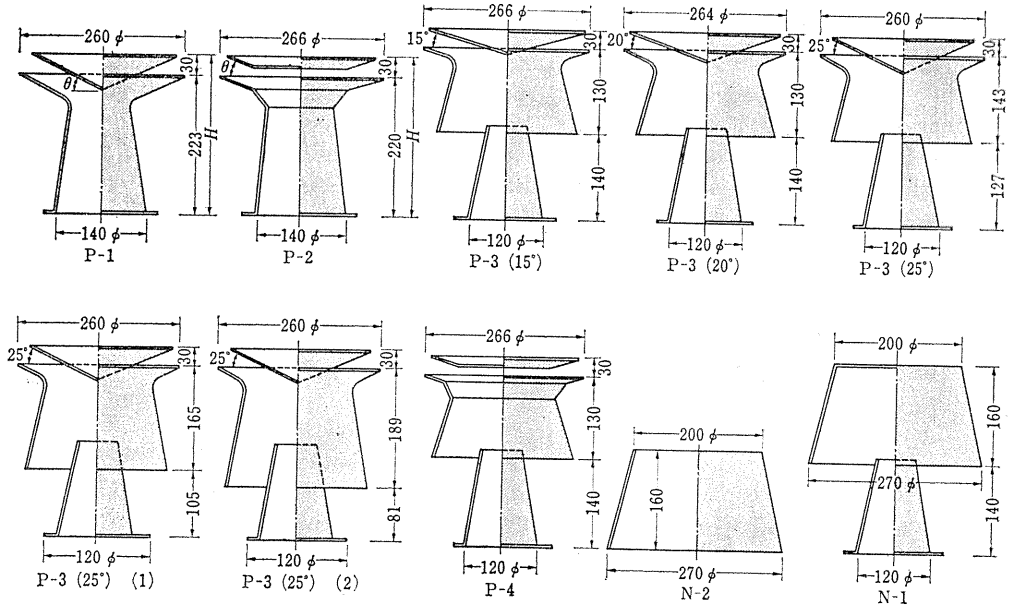

Fig. 6. Experimentally-made air outlets for model tests (Left-hand side shows cross section and right-hand side elevation. Discharge angle θ and height H in both Type P-1 and Type P-2 are freely adjustable.)

4. 2. 1. Characteristics Tests of Single Air Outlets

Such characteristics as static pressure losses, inductive performance, velocity profiles and centerline velocity constants of single air outlets under isothermal conditions were obtained. Since in isothermal tests the velocity distribution would

be similar except in the vicinity of wall surfaces regardless of the size of models and air velocity at the outlet, consideration of dimensionless numbers was not made in particular.

(1) *Static Pressure Losses*

Measurement of static pressure losses was made by connecting the straight section of a duct to the air outlet and using a Pitot tube. A part of the test results is indicated in Fig. 7.

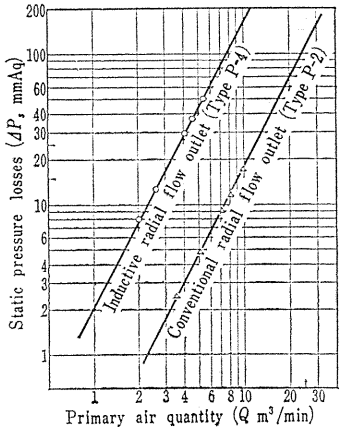

Fig. 7. Static pressure losses.

(2) *Induction Performance*

Inductive ratio is calculated by equation (10).

$$k=\frac{Q_i}{Q_P}\times 100=\frac{Q_T-Q_P}{Q_P}\times 100 \tag{10}$$

k=induction ratio

Q_P=primary air volume (m³/h)

Q_i=induced air volume (m³/h)

$Q_T=Q_P+Q_i$=total air volume (m³/h)

As shown in Fig. 8, inductive performance of the induction type outlets were measured using air chamber whose static pressure was adjusted to keep the same with the outside atmospheric pressure by adjusting the damper for various dimensions of A and Ho in Fig. 8. The results are given in Fig. 9. As is clear from the figure, the primary air volume Q_P is expressed as a logarithm of the secondary air velocity V_o.

(3) *Velocity Profile*

Fig. 10 and Fig. 11 show the velocity profiles of induction nozzle type outlet and inductive radial flow type outlet respectivery, while Fig. 12 shows that of conventional radial flow outlet. As is known from these figures, the spread angle of the flow from the inductive radial flow outlet is about 30 degrees whose Ho is between 20 mm and 30 mm.

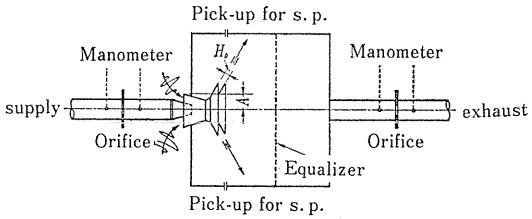

Fig. 8. Mesurement of induced air volume.

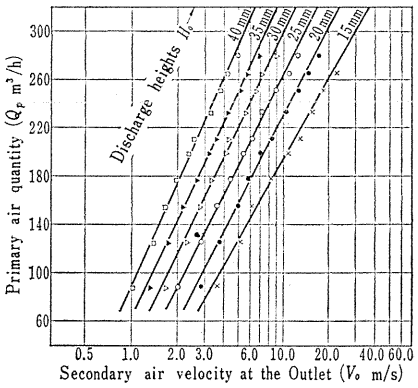

Fig. 9. Primary air quantity and secondary air velocity at outlet. (Type, P-3, 25°)

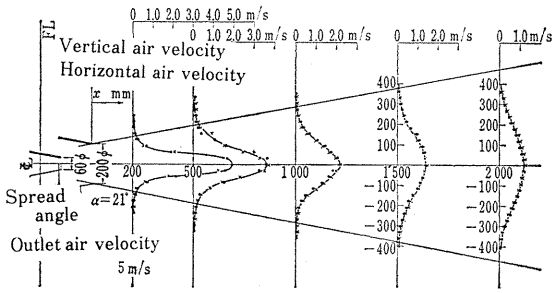

Fig. 10. Velocity profile of induction nozzle outlet. (N-1)

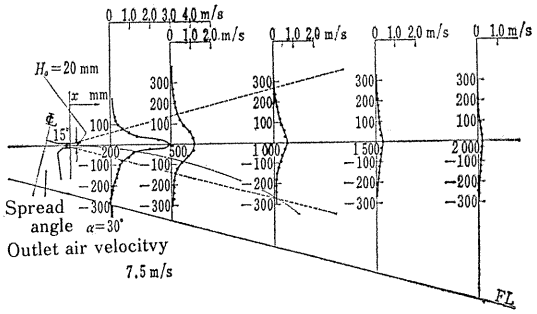

Fig. 11. Velocity profile of induction radial flow outlet. (P-4, Ho=20mm)

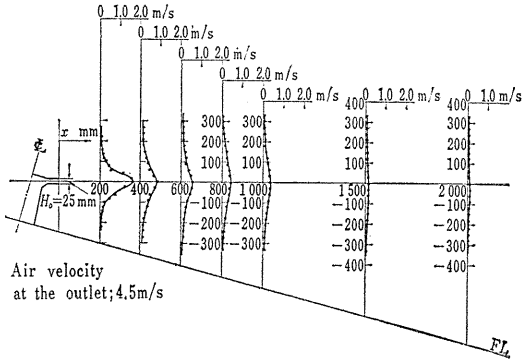

Fig. 12. Velocity profile of conventional radial flow outlet. (Type P-2)

(4) *Centerline Velocity Constant*

Fig. 13 shows the test results of the centerline velocity constants of a radial flow outlet. According to the experimental results, the centerline velocity constant K of a radial flow outlet lies within the range of 3.2 and 3.7 and does not vary appreciably depending on the discharge angle, height and shape of the outlet. However, the values are larger in the conventional type than in the induction type.

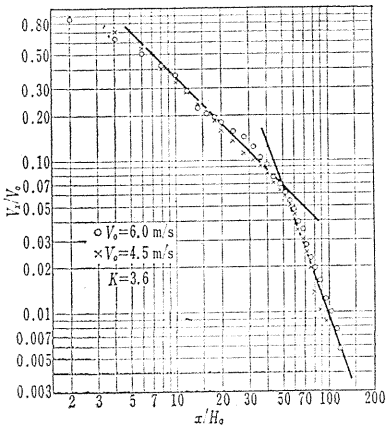

Fig. 13. Centerline velocity constants of radial flow outlet Type P-1 (30°), H_o=25mm.

4. 2. 2. Experiments on Air Distribution in Room

These experiments consisted of tests with models to find air distribution in the room cooled under non-isothermal conditions and a supply outlet was disposed at the center of the circular floor of the dome. The air velocity at the outlet of the model was obtained from Eq. (8) and the air volume was computed on the basis of this value and the area of the outlet. Inner heat generation from the audience of 1,000 persons and illumination was reproduced from Eq. (9). As a means of heat generation in the model an electric potential was applied to an electric conductive paper which was effective as a planar heat-producing body. Adjustments were made in this manner to obtain a steady state balance among those of the heat externally supplied, internally generated heat and the chilled air discharged into the model.

Since the outlet and inlets were arranged symmetrically with relation to the center, measurements of temperatures and air velocities at various points within the model were made only for one-half of a cross section of the dome, or in other words for only a quater sphere. Measurements taken on this representative cross section are applicable to all sections passing through the center. Temperature measurements were made with copper-constantan thermocouples while air velocity measurements were made with thermocouple-type hot wire anemometers. Among the test results, temperature and air velocity distributions for Type P-1 (conventional radial flow outlet) are indicated in Fig. 14 and Fig. 15. In the series of model experiments, local details such as the shape of plaque of outlet were found to have little influence on air distribution in the case of simple radial flow outlets. When the air velocity at the outlet was raised there was some increase in the difference between the upper and lower air velocity distributions. With the inductive radial flow outlets, the larger the discharge angle, the more the uniformity of temperature distribution in the occupied zone could be maintained except for a partial area near the center of the circular floor. A comparison between the conventional radial flow type and the inductive radial flow type proved that the temperature difference between the upper and lower parts was large with the former and small with the latter.

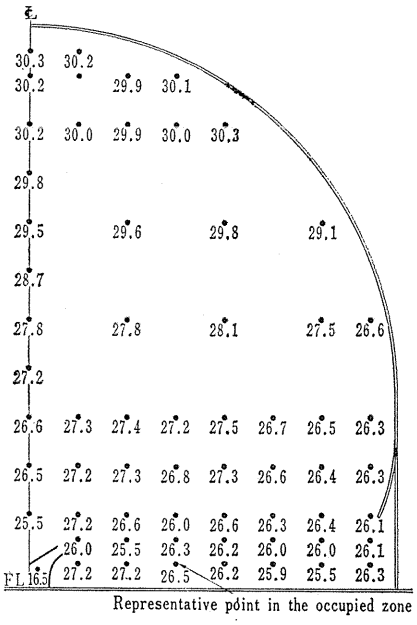

Fig. 14. Temperature distribution by scale model experiments P-1 (30°), (℃).

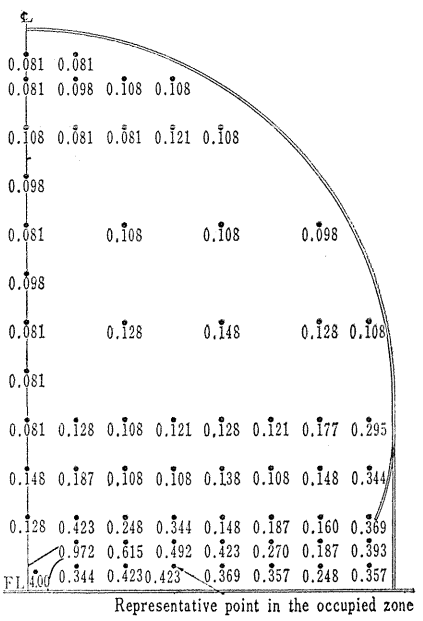

Fig. 15. Air velocity distribution by scale model experiments P-1, (30°), (m/s).

It is considered such a result is due to the difference in ventilation rates between these types. Although it was decided not to adopt axial flow outlet (Type N-1), from the standpoints of air velocity at the surface of the screen at the top, and of lack of economical feasibility and energy saving, it was ascertained that "membrane cooling" could be achieved with this type as anticipated, though it was not shown in the figures. Fig. 16 shows the state of the air distribution test using smoke.

From the series of model tests it was clarified that a conventional radial flow

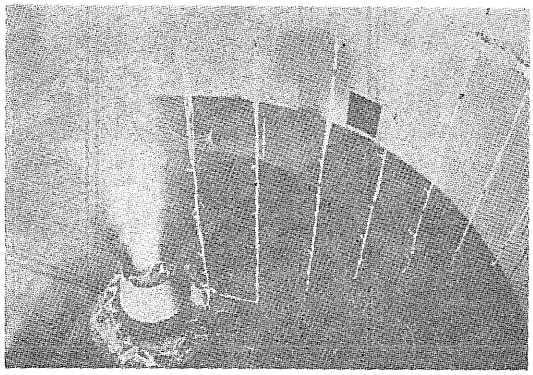

(n_l=1/10, $n_{\Delta t}$=1.65, n_v=0.406)

Fig. 16. State of the distribution test for N-1 type.

outlet (Type P-1) was most suitable for the Midori Pavilion as it could attain economization of the air-conditioning system with locally limited cooling effect of the occupied zone only, uniformity of temperature and air velocity in the occupied zone, reduction of noise generated at the supply outlet, and saving of works on the outlet such as fabrication, delivery and installation. The actual shape of this outlet was such that the discharge angle was 30 deg with height of 150 cm and air velocity at the outlet 4.0m/s. A detailed view of the outlet adopted is given in Fig. 17.

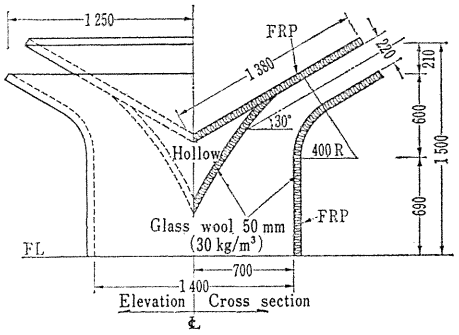

Fig. 17. Detailed view of outlet adopted (mm).

4. 3. Actual Measurements and Comparison with Model Experiments

4. 3. 1. Outline of Actual Measurements

In the last part of July 1970 when the cooling load characteristics of the actual Midori Pavilion had settled down to be roughly the same as those of the experiments, measurements were made on air temperature distribution and air flow direction inside the actual pavilion. These measurements were performed when the temperature difference between the outlet and the occupied zone reached 10 deg as in the model experiments, while the "Astrorama" were projected on the screen 6 times between 9 hrs and 13 hrs. Measurements of temperature and air velocity were made with (C_u-C_o) thermoconples and an electronic data recorder and with a hot wire anemometer respectively.

4. 3. 2. Result of the Measurements

(1) *Temperature Distribution*

The comparison of actual measurements is given in Fig. 18 and Fig. 19. In these figures, two temperature values are indicated for each measurement point, the upper representing the actual measurement values and the lower the model experiment values. As is clearly seen in figures these temperature distributions in the vertical direction are in quite good agreement with each other. However, regard to the temperature distribution in the horizontal direction of the occupied zone, it is fairly high in the perimetric area in the case of the actual measurements in both cases. This is considered due to the fact that, although lights in the dome were turned off since films were being projected during the actual measurements, very little time had elapsed after the turn-off of lights and the residual load of the illumination lamps gave rise to high temperatures.

(2) *Air Velocity Distribution and Flow Direction*

The results of air velocity distribution in the occupied zone are shown in Fig. 20. For each measurement point the upper value represents the actual measurement results whereas the lower value represents the model experiment results. As is evident from the figure, the actual measurement values are smaller as a whole, and the velocities are below 1m/s. Therefore, the precision of the anemometer

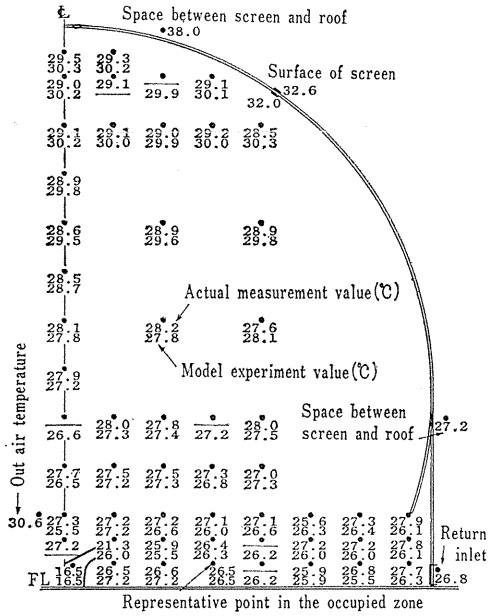

Fig. 18. Comparison of actual measurements of temperature distribution with model experiments. (The upper represents the actual measurement values and the lower the model experiment values)

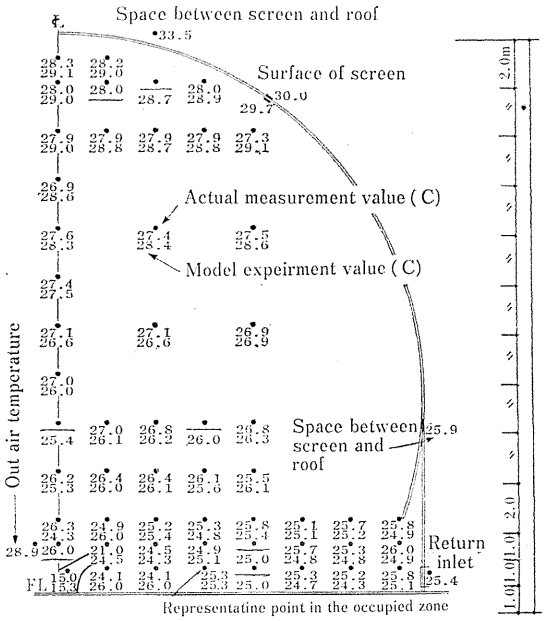

Fig. 19. Comparison of actual measurements of temperature distribution with model experiments No. 2 (9; 40-9: 48 on projection, 1060 spectattors).

brings about a problem and it is difficult to give a correct judgment. The air flow direction within the dome usiug dandelion tufts is shown in Fig. 21.

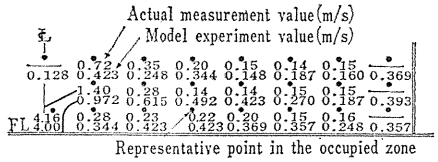

Fig. 20. Comparison of actual measurements of air velocity distribution with model experiments in occupied zone.

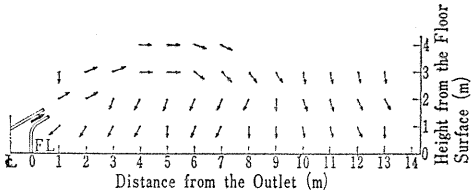

Fig. 21. Air flow direction in occupied zone.

4. 3. 3. Evaluation of the Results

(1) The temperature distribution both in the occupied zone and in the upper zone shows fair agreement between the model and the actual except for the peripheral area, where the residual effect from the lights during projection is considered to give higher temperature in the actual case.

(2) The air temperature around the outlet in the model measurements is considerably higher than that in the actual case. This may be considered partly due to the delicate difference in the discharge direction and partly due to the radiant effect on the thermocouples from the surface of the outlet made of steel in the model and FRP insulated inside in the actual.

(3) Air velocity distribution shows a little difference between the model and the actual mainly because of the difficulty of measurements in low velocity and partly because of insufficient precision of the anemometer; the similarity theory should not simply be claimed for its error as shown in these comparisons.

(4) It was disclosed that the occupied zone air-conditioning to seek an economical feasibility and energy conservation could be satisfactorily applied to the air-conditioning of large spaces.

(5) The similarity theory for air distribution between the model and the actual based on matching of the Archimedes Numbers proved to be quite satisfactory and reliable.

(6) It was proved that the induction type of outlets, both the nozzle and the plaque, showed good performance for the air distribution in large spaces, and that such characteristics as velocity distribution and centerline velocity constant were peculiar compared with non-induction type of outlets.

5. The Case of Kuramae-Kokugikan (Sports Arena)

5. 1. Outline of Building

5. 1. 1. Outline of Architecture

The Kuramae-Kokugikan is the sports arena for Sumo (Japanese style wrethling), and the air-conditioning systems were newly applied in 1971. The number of persons admitted is about 12,000. The outline of the building is as follows:

Structure: Reinforced concrete, Two stories

Maximum height above ground level: 25.2 m

Building area: 6,026 m²
Total floor area: 10,830 m²

Fig. 22 shows the plan of ground floor, and Fig. 23 shows the section of the building.

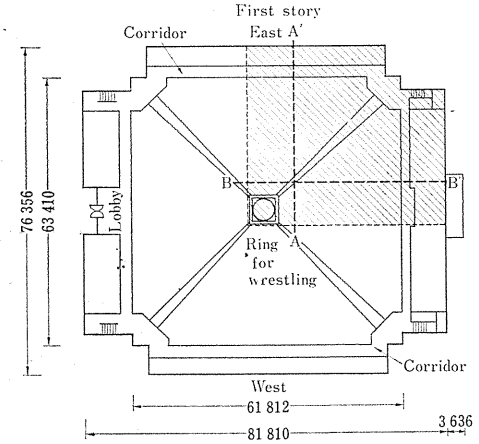

Fig. 22. Plan of the Kuramae-Kokugikan (mm).

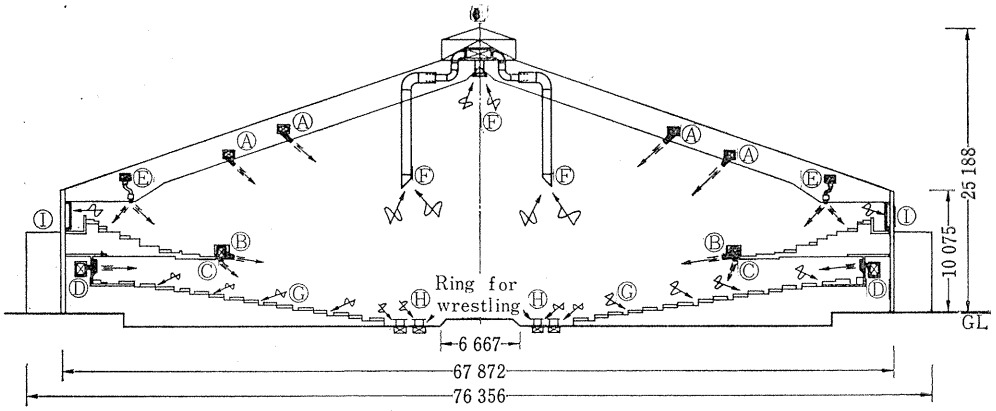

Fig. 23. Section of the Kuramae-Kokugikan.

5. 1. 2. Outline of Air-Conditioning System

In this case, the air-conditioning zone was restricted to the occupied zone also. In order to remove the heat from the lights in the upper space, smoke and dust which are generated from spectators in the occupied zone, the system shown in Fig. 1(a) was employed.

The re-blown air into the upper zone at the rate of 20 percent of return air volume from the occupied zone is exhausted to outside through the inlets in the ceiling. Ⓐ and Ⓕ in Fig. 23 indicate the outlets and inlets respectively in this ventilation system for the upper zone. Thirty-six circular nozzles (Ⓑ in Fig. 23)

were provided at the end of the second floor balcony, and the discharge angle of these nozzles can be adjusted freely. The air-conditioning system for the interior zone of the ground floor was divided into four sub-systems, while the perimeter zone into two. At the second floor, there are two sub-systems in the air-conditioning. The design temperature of the occupied zone is 26℃ and 21℃ each in summer and in winter respectively.

The temperature difference between air outlets and the representative point in the occupied zone (Δt) is fluctuated with the numbers of occupied person and meteorological conditions, the average value being 7 to 9 deg. C in cooling, 6 to 8 deg. C in heating and 10 deg. C in preheating before occupancy starts. When numerous number of persons are seated, cooling operation is required even in heating season. The data on heat load and ventilation of the air-conditioning system are shown in Table 3. An inside view of the building is shown in Fig. 24.

Table 3. Data on heat load and ventilation of the air-conditioning system for the Kuramae-Kokugikan.

Room Cooling Load (peak load)		1,448,000 Kcal/h
Room Heating Load (preheating load)		444,000 Kcal/h
Outside Air Load	in cooling	774,000 Kcal/h
	in heating	1,623,000 Kcal/h
Apparatus Cooling Load		2,352,000 Kcal/h
Apparatus Heating Load		2,167,000 Kcal/h
SHF in cooling		0.68
Air Volume	for occupied zone	439,000 m^3/h
	for upper zone	72,000 m^3/h
Room Cooling Load per unit floor area		134 $Kcal/m^2h$
Room Heating Load per unit floor area		41 $Kcal/m^2h$
Air Volume (for occupied zone) per unit floor area		41 m^3/m^2h
Air Change		10/h

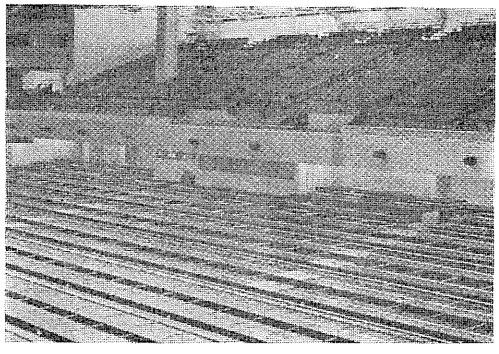

Fig. 24. Inside view of the Kuramae-Kokugikan.

5. 2. Scaled Model Experiments

5. 2. 1. Outline of Scaled Model

As the arena was symmetrically designed for both east-west axis and north-south axis, the air distribution in each quarter could be regarded as the same. So the model was made only for a quarter of the arena. The reduction scale was 1/12. A quarter portion of the model is shown by shaded area in Fig. 22 and the locations of two representive sections for showing temperature distribution measured are shown by broken line.

Measuring points in each section are shown in Fig. 28.

The model was made of 9 mm thick wooden panel, and the two imaginary walls are provided as indicated by the dotted line in Fig. 22, with sufficient insulation of 50 mm thick glass wool. Fig. 25 shows an inside view of the model. In these model experiments the average temperature difference was maintained to be 7.7 deg. C in cooling and 6 deg. C in heating, and the reduction ratio of temperature difference (Δt) was confined to 3.0 in cooling and 2.0 in heating as shown in Table 1. The representative point of the occupied zone was taken at the center of the ground floor as indicated in Fig. 28. As the means to generate the inside heat generation from spectators and illumination in the model, an electric conductive paper was employed as described in *4. 2. 2.*

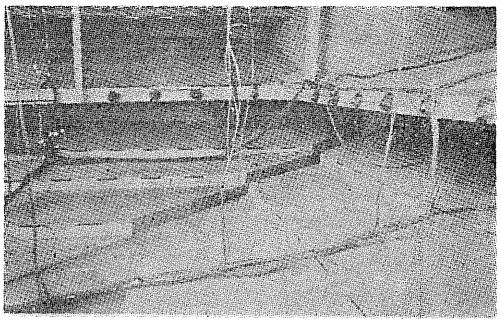

Fig. 25. Inside view of the scaled model.

5. 2. 2. Experiments on Air Distribution within the Room

(1) *Air Distribution in the Case of Cooling*

Model experiments were performed with circular nozzles having the discharge angle varied, with or without operation of circulating (secondary) ventilation system in the upper zone. Fig. 26 and Fig. 27 show the temperature distribution in cooling with the discharge angle of 20° for the circular nozzles, with or without operation of circulating ventilation.

Fig. 28 shows the air velocity distribution in cooling obtained from experiments. Temperature distribution in the occupied zone was recognized to be almost uniform with the exception of rear seats on the second floor. Air velocity distribution was also satisfactory in almost all places within the occupied zone, without any cold draft. Further, considering the temperature difference brought about between the upper zone and the occupied zone as shown in these figures, the cooling performance restricted to the occupied zone was fairly successful.

(2) *Air Distribution in Heating*

Fig. 29 and Fig. 30 show the temperature distribution in heating with the circulation nozzles at 50° discharge angle, with or without operation of circulating ventilation in the upper zone. It was recognized that an uniform temperature

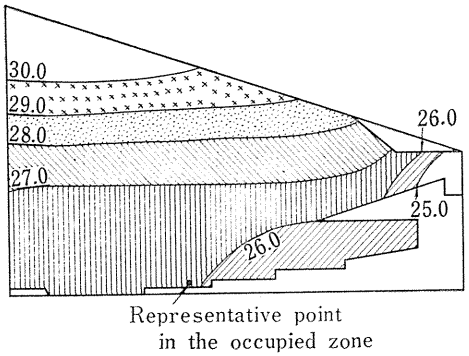

Fig. 26. Temperature distribution in cooling from the model experiments, with circulating ventilation. (℃) (Δt=7.7 deg)

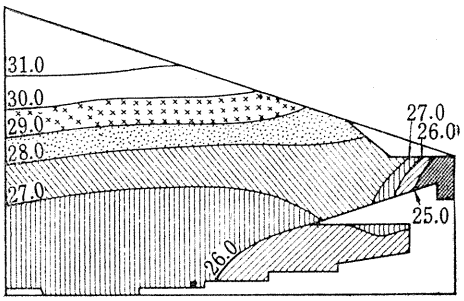

Fig. 27. Temperature distribution in cooling by model experiment (℃), without circulating ventilation. (Δt=7.7 deg)

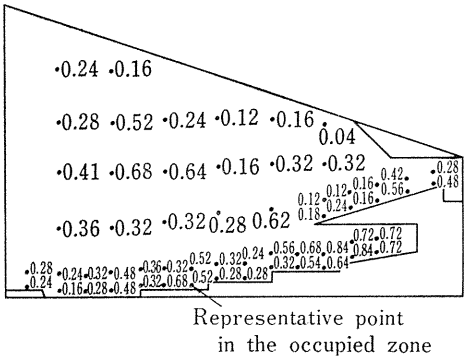

Fig. 28. Air velocity distribution in cooling from the model experiments (m/s), with circulating ventilation. (Δt=7.7 deg)

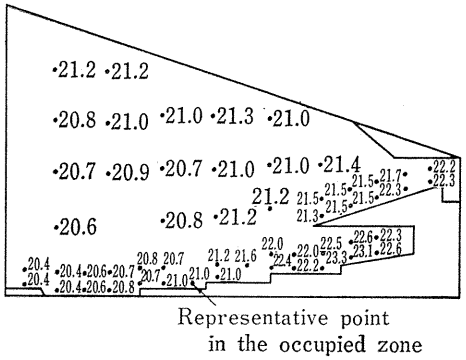

Fig. 29. Temperature distribution in heating by model experiment (℃), with circulating ventilation. (Δt=6 deg)

Fig. 30. Temperature distribution of the model experiments in heating (℃) (Δt=6 deg. Circulating ventilation: off)

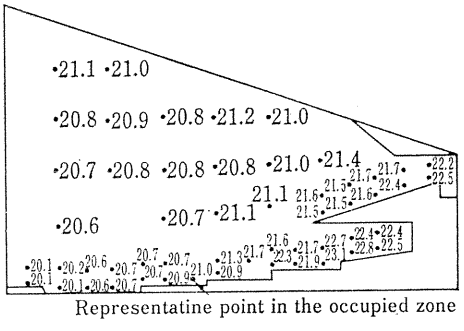

distribution was obtained also in the case of heating. In these figures the air temperature in the upper zone are almost equal to the one in the occupied zone. As the warm air heating system usualy tends to cause a considerable temperature difference between the upper and the lower, this attempt of the occupied zone heating can be considered as successful. Little difference of temperature distribution was recognized in the case of heating bteween with and without operation of circulating ventilation system in the upper zone.

5. 3. Actual Measurements and Comparison with Model Experiments

3. 3. 1. Outline of Actual Measurements

The actual measurements for temperature and air velocity distribution were conducted after completion of the building, in January for heating conditions, and in May and September for cooling. The cross section of A–A' in Fig. 22 was taken in the actual measurement which is the same section as taken in the model experiments.

5. 3. 2. Results of Measurements

(1) *Temperature Distribution*

Fig. 31 and Fig. 32 show the comparison of temperature distribution in heating conditions between the actual and the model. The temperature difference (Δt) was 6. 0 deg. C which was equal to the value of model experiments. In these figures, two temperature values are indicated for each measurement point, the upper

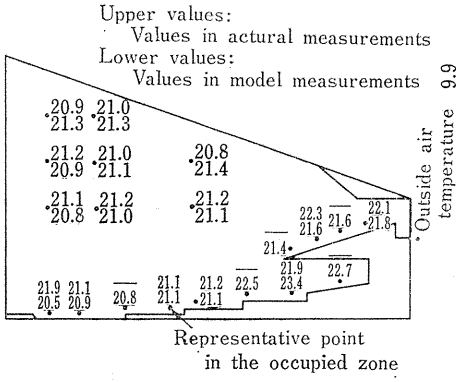

Fig. 31. Comparison of actual measurements of temparature distribution in heating with model experiments (℃) (Δt=6 deg, Circulating ventilation: on)

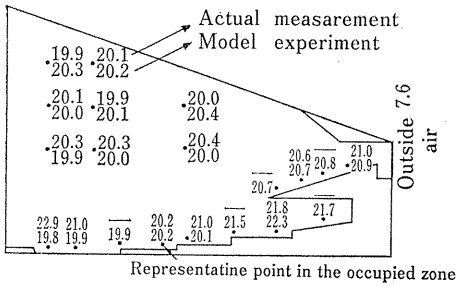

Fig. 32. Comparison of actual measurements of temperature distribution in heating with model experiments. (℃) (Δt=6 deg, Circulating ventilation: off)

represents the actual measurement values and the lower the model experiment values.

As is clearly seen from these figures, both of the temperature distribution are in quite good agreement with the experimental results except for the values in the center of the arena. The disagreement thus appeared is supposed to be caused by

the radiant floor panel heater provided in the center part of the actual arena which was omitted at the model experiment due to the difficulty of establishing the similarity conditions for radiant heat transfer.

(2) *Air Velocity Distribution and Flow Direction*

Air velocity distribution in the cooling season is shown in Fig. 33. Air flow direction actually measured in the occupied zone is shown in Fig. 34.

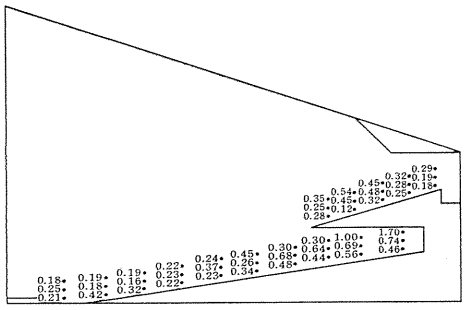

Fig. 33. Air velocity distribution in the cooling season from actual measurement.

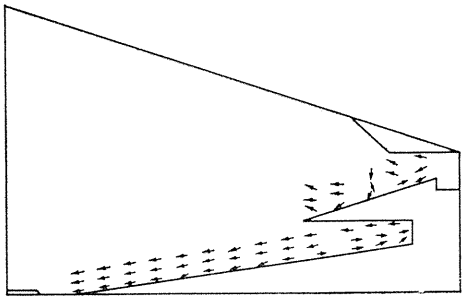

Fig. 34. Actual measurement of air flow distrbution. (section A—A′)

5. 3. 3. Evaluation of the Results

(1) Prediction of air distribution in the occupied zone air-conditioning in the Kuramae-Kokugikan with scaled model was performed backed up by the fair results on the Midori Pavilion, and the result was quite satisfactory to verify the similarity theory and the advantage of the occupied zone air-conditioning.

(2) It was proved that the secondary air circuit by reused air for the upper zone in large spaces, which contain lots of dust and smoke of cigarettes, was very effective in preventing the conditioned air in the occupied zone from uprising to the upper space, and in removing dust and smoke to outside.

(3) The fact that the temperature of both the upper zone and the occupied space were almost equal each other in heating season, shows success of the occupied zone air-conditioning even in warm air heating.

6. The Case of M-Factory

6. 1. Outline of Building

6. 1. 1. Outline of Architecture

This factory, in which large precises machines are assembled, was constructed in March, 1972. The outline of the building is as follows:

Structure: Steel frame, One story

Wall material: Pre-cast light-weight concrete panels

Maximum height above ground level: 26.9 m

Building area: 2, 323 m²
Total floor area: 2, 576 m²
Fig. 35 and Fig. 36 show the plan and cross section of the building respectively.

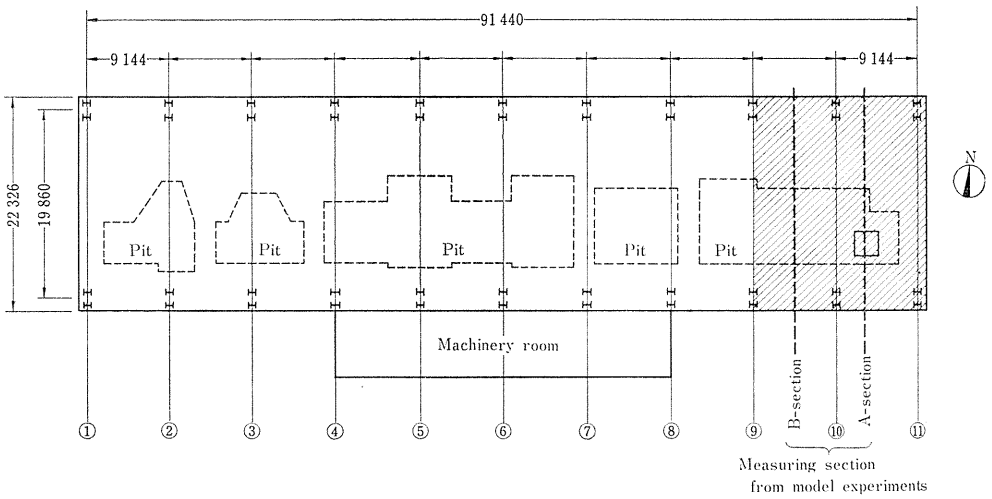

Fig. 35. Plan of M-Factory manufacturing large precise machines (mm).
(the total area of building: 2324 m²)

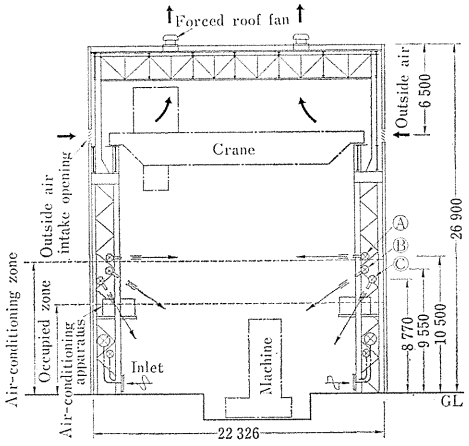

Fig. 36. Section of the Factory (mm).
(Ⓐ, Ⓑ, Ⓒ show the air outlets)

6. 1. 2. Outline of Air-Conditioning System

A uniform temperature distribution with a range of 2. 0 deg. C in the occupied zone (within 7 meters above floor surface) was strictly required for accurate assembling of large precise machines. The air supply system, therefore, was divided into three as shown in Fig. 36. For safety, air-conditioning zone, i, e, the occupied zone, was decided to be 10 meters above the floor. In Fig. 36 discharge

air temperature at the outlets Ⓐ is equal to that of the systems Ⓑ Ⓒ in cooling cycle, while in heating, it is equal to the room air temperature as the return air from the occupied zone is directly reused. Special induction type of air outlets which is shown in Fig. 37 were developed to bring about the air movement around outlets and wall surfaces.

Data on heat load and ventilation are shown in Table 4, and various characteristics of outlets are shown in Table 5. As the ventilation system for the upper zone, the type (b) in Fig. 1, which use the outside air, was adopted, because the operation of it can be stopped in winter due to the little oil smoke to be generated.

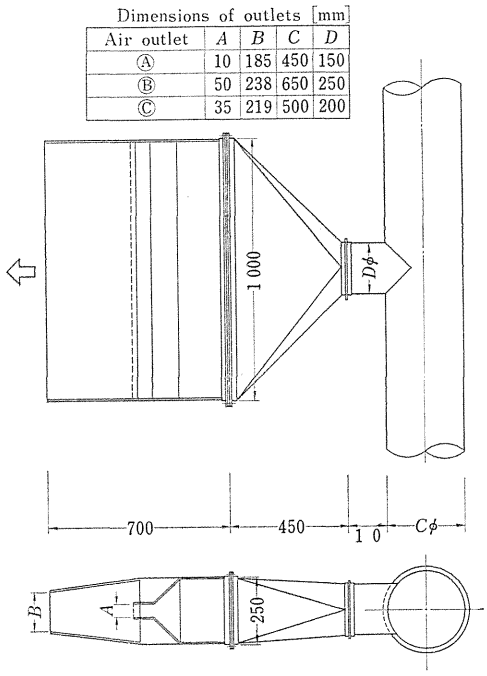

Fig. 37. Air outlet of induction type.

Table 4. Data on heat load and ventilation of the air-conditioning system for M-Factory.

Room Cooling Load		372, 100 Kcal/h
Room Heating Load		188, 000 Kcal/h
SHF (in cooling)		0.988
Outside Air Load	in cooling	88, 500 Kcal/h
	in heating	60, 000 Kcal/h
Apparatus Cooling Load		506, 700 Kcal/h
Apparatus Heating Load		273, 000 Kcal/h
Primary Air Volume		103, 200 m^3/h
Room Load per unit floor area		160 $Kcal/m^2.h$
Air Volume per unit floor area		45 $m^3/m^2.h$
Air Change		4.5/h

Table 5. Various characteristics of the outlets in M-Factory.

Symbol of Outlets	Numbers of Outlets	Primary Air Volume (m^3/h)	Primary Air Velocity (m/s)	Secondary Air Quantity (m^3/h)	Primary Air Temperature Difference (Δt) in Heating (deg)	Primary Air Tempreature Difference (Δt) in cooling (deg)
Ⓐ	80	375	10.4	1,030	8—10	0
Ⓑ	40	1,220	6.8	1,930	8—10	6—8
Ⓒ	40	610	4.9	1,190	8—10	6—8

6. 2. Scaled Model Experiments

6. 2. 1. Outline of Scaled Model

While a complete model of the factory would be too large to attain accurate data, the scale had to be less than 1/50 from the capacity of the test room. Now in this factory, as the shape of the structure, air-conditioning systm and arrangements of air outlets and inlets are similar each other every span, the span of ⑨～⑪ in Fig. 35 were adopted for the test model. The linear reduction ratio of 1/10 was thereby secured, which was thought satisfactory for the accuracy of model experiments. Two representative sections to be measured for temperature distribution in the factory are shown with broken line in Fig. 35.

Since the outlets and inlets were located symmetrically, the measurements of temperature and air velocity at various points shown in Fig. 45 were conducted only for one-half of the cross section of Fig. 36. The model was made of wood. The wall surface which was created from sampling two spans only for experiment (⑨ row in Fig. 35) was insulated sufficiently with 50mm thick glasswool.

To simulate inside heat generation from machines (61,000 kcal/h in the space between ⑨～⑪ span in the actual building, an electrically heated nichrome wire was applied. The nichrome wire was wrapped with aluminium foil to prevent radiant heat transfer to thermocouples during the temperature measurements.

In this model experiments all procedures were carried out with $n_{\Delta t}=1$, because it was difficult to assume a large temperature difference between primary air temperature at the outlets and the room air temperature at the representative point in the occupied zone, due to its large air volume of the model. Temperature and air velocity measurements were made using the same operations described in *4. 2. 2.* Further, it was supposed that, in the actual, 32℃ of outside air was flowing into the upper zone through the upper ventilation openings with 1.72 m/s of average velocity in the case of summer cooling. Model experiments were performed with the temperature difference (Δt) varied, with or without circulating secondary ventilation in the upper zone.

6. 2. 2. Experiments on Room Air Distribution

(1) *Temperature Distribution in Cooling*

Among the results of experiments in cooling, temperature distribution in the case of 10 deg. of temperature difference (Δt) between the outlets and the representative points in the occupied zone, with and without inside heat generation from machines, are shown in Fig. 38 and Fig. 39 respectively. In these tests, the circu-

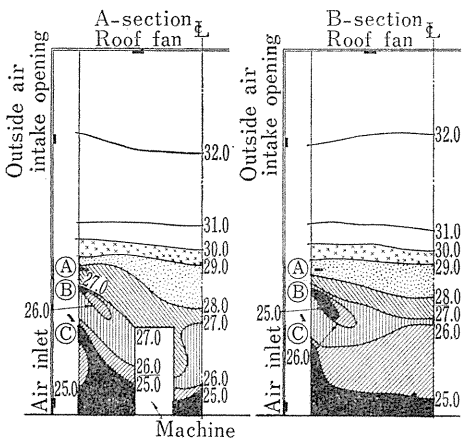

Fig. 38. Temperature distribution in cooling with heat generation from inner machines by model experiments (℃). (Δt=10 deg)

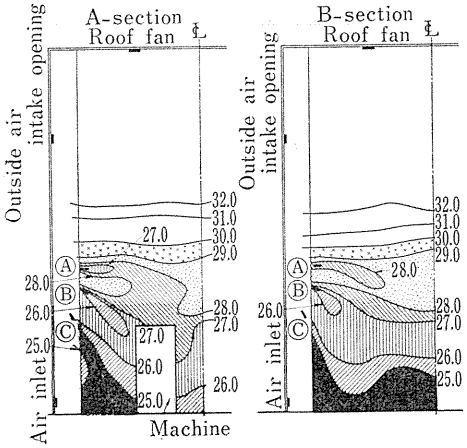

Fig. 39. Temperature distribution in cooling without heat generation from inner machines by model experiments (℃). (Δt=10 deg)

lating ventilation system was operated.

The temperatures of various points in the occupied zone within 7 m above the floor are found within 2 deg. of the range. While, the air temperature of the upper zone without inside heat generation was found a little higher than that with inside heat generation. This is because heat gains from the outside was naturally larger in the case without inside heat generation, the temperature difference (Δt) being maintained equal in both cases.

When the roof ventilation fans were off, the temperature of the upper zone was recognized to rise by about 1.0 to 1.6 deg. Fig. 40 depicts how the occupied zone and the upper zone are separated each other visually in stratification.

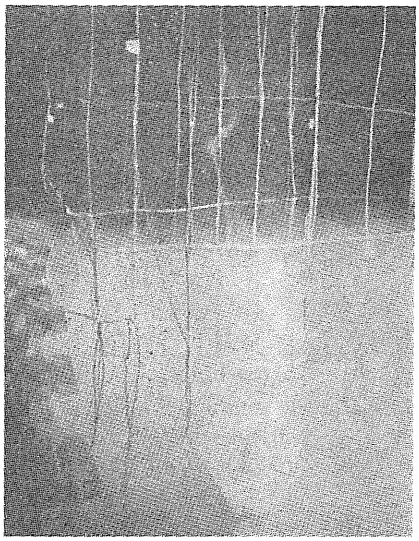

Fig. 40. State of the air distribution test.

(2) *Temperature Distribution in Heating*

Fig. 41 and Fig. 42 show the temperature distribution in heating with the temperature difference (Δt) varied with inside heat generation. Since the rate of inside heat generation is the same in each case, the difference in Δt is regarded proportional to that of heat loss to the outside. In heating cycle the temperature of the outlets Ⓐ in Fig. 36 was maintained equal to the temperature of the occupied zone.

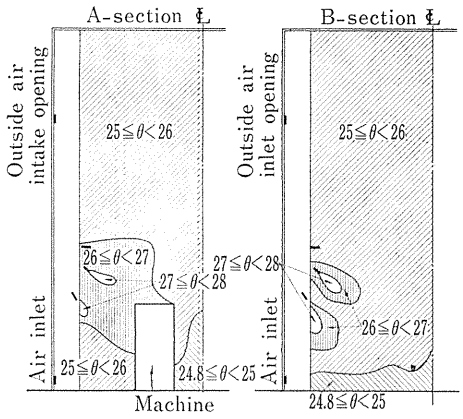

Fig. 41. Temperature distribution in heating with heat generation from inner machine by model experiments (℃). (Δt=10 deg)

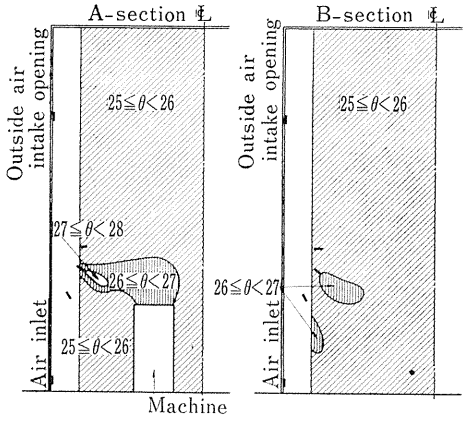

Fig. 42. Temperature distribution in heating with heat generation from inner machine by model experiments (℃). (Δt=6 deg)

Fig. 43 shows the temperature distribution in heating when Δt is 10 deg. without inside heat generation. In any case of heating it was proved that the uniform temperature distribution in the occupied zone was obtained and the temperature difference between the upper zone and the occupied zone was found almost none. The uniform temperature distribution in the occupied zone as realized is considered due to the separation of the air supply system into three parts, the adoption of the special induction type air outlets, the minimization of Δt and the reduction of heat load from outside by increasing heat resistance of exterior walls and roof.

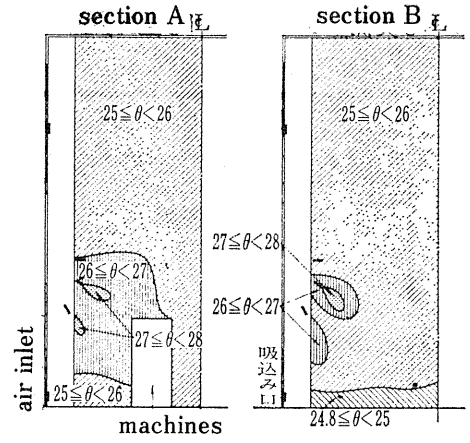

Fig. 43. Temperature distribution in heating without heat generation from inner machines by model experiments (℃). (Δt=10 deg)

6. 3. Actual Measurements and Comparison with the Model Experiments

6. 3. 1. Outline of Actual Measurements

In August of 1972 and March of 1973, when the cooling and heating loads of the actual building was reduced to be roughly the same as those of the experiments, measurements in the actual factory were made on air temperature and velocity distribution. The temperature difference between the outlets and the occupied zone (Δt) reached the same value as in the model experiments.

The C-section of Fig. 35, the same as B-section, was chosen for the measurements on the distribution of both temperature and air velocity, and the A-section was employed for measurements of velocity additionally.

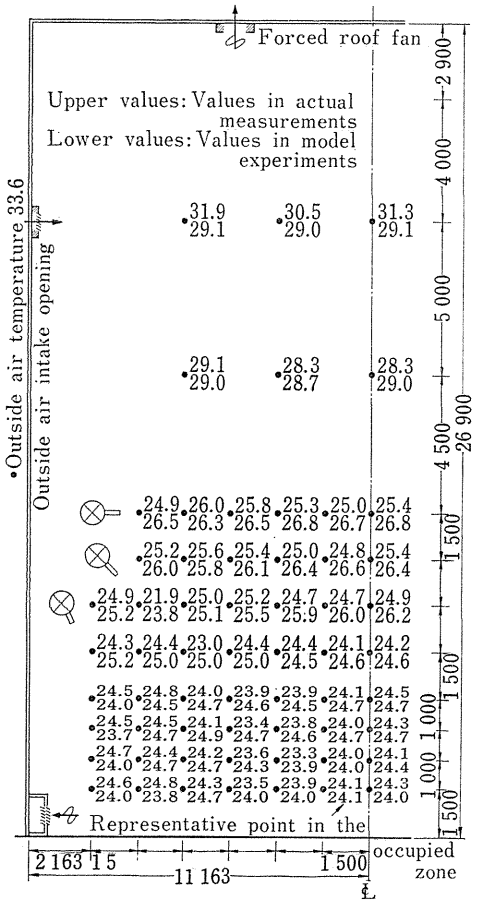

Fig. 44. Comparison of actual measurements of temperature distribution in cooling with model experiments (℃), with inner heat generation. (Δt=7.4 deg)

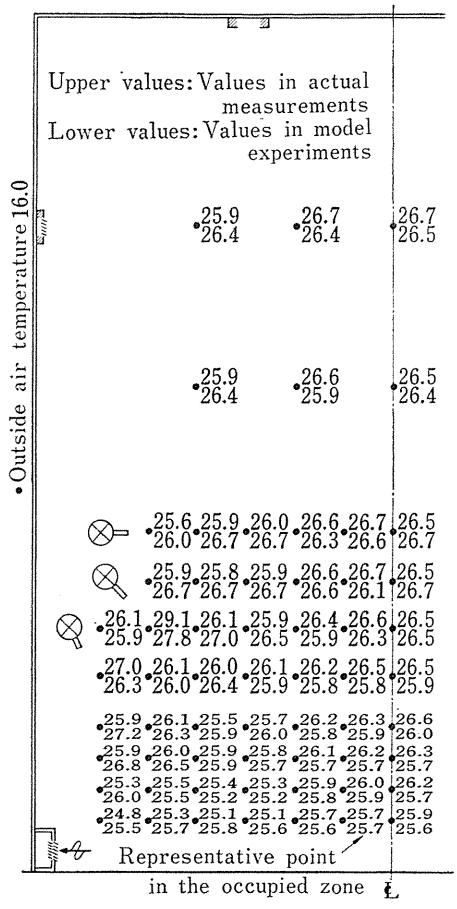

Fig. 45. Comparison of actual measurements of temperature distribution in heating with model experiments (℃), with inner heat generation. (Δt=6.5 deg)

6. 3. 2. *Results of Measurements*

(1) *Temperature Distribution*

The comparison of temperature distributions between the actual and the model experiments are shown in Fig. 44 to indicate cooling conditions with inside heat generation, and in Fig. 45 and Fig. 46 to indicate heating conditions with and without inside heat generation respectively. The meaning of two temperature values in these figure is explained in *4. 3. 2.*

As is clearly seen in these figures, the temperature distribution is in quite good agreement with each other. The temperature in the upper zone, however, is found generally somewhat higher in the actual than that in the model. This difference is considered to be caused by the radiant heat from the lights provided beneath the ceiling to the thermocouples used for the measurements.

(2) *Air Velocity Distribution*

Fig. 47 shows the air velocity distribution of A-section in isothermal conditions for reference.

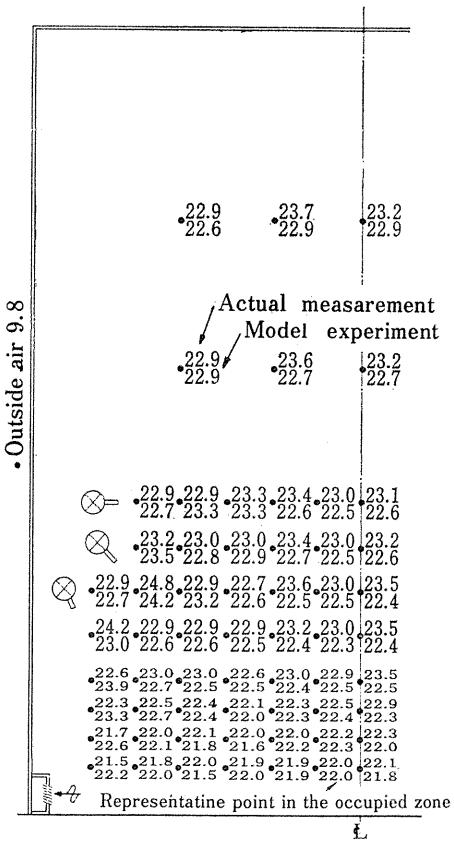

Fig. 46. Comparison of actual measurements of temperature distribution in heating with model experiments (℃). (Δt=10 deg, without inside heat generation)

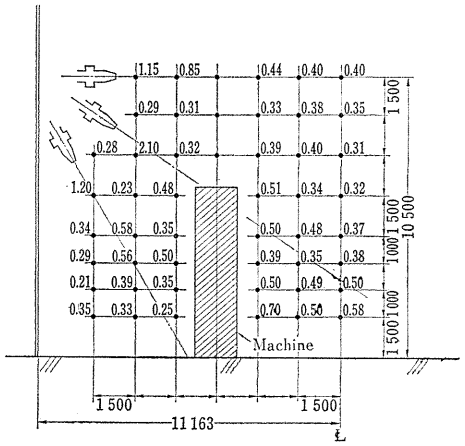

Fig. 47. Air velocity distribution from the actual measurements (m/s). (A-cection, in isothermal condition)

6. 3. 3. Evaluation of the Results

(1) In the comparison between the model experiments and the actual measurements, good agreement was recognized similarly to the cases of Midori Pavilion and Kuramae-Kokugikan. This fact may lead to the conclusion that the similarity theory of modeling is fairly reliable.

(2) It is proved that the occupied zone air-conditioning can be realized within 1.0 deg. C of the range for the occupied zone of large spaces.

(3) Similarly with the case of the Kuramae-Kokugikan, the occupied zone heating system which utilizes warm air is considered efficiently achieved judging from the fact that the air temperature between the upper zone and the occupied zone is almost equal.

7. Calculation Method of Cooling Loads for the Limited Occupied Zone Air-Conditioning

7. 1. Outline of Calculation Method

A calculation method for cooling loads for the occupied zone air-conditioning is proposed hereinafter. The new calculation method is unique in taking account of radiant heat from non air-conditioned spaces, and heat gain associated with what is called imaginary air exchange between air-conditioned space and non air-conditioned space caused by induction and mixing effects of the discharged air.

As shown in Fig. 48, the walls enclosing the large space is divided into two parts for convenience, the walls in the non air-conditioned upper zone including the ceiling surface and the walls in the air-conditioned occupied zone including the floor surface. The radiant heat exchange among the wall surface can be calculated exactly by using the absorption factors proposed by Gebhart 4). For simplicity the radiation upon the surface is assumed entirely transfered to the space by convection as shown in Fig. 48, where the absorptivity of the walls is assumed 1.0 and the angle factors between walls in two zones 1.0, for deriving simpler equation forms. The explanation of the symbols used in equations are shown in Table 6.

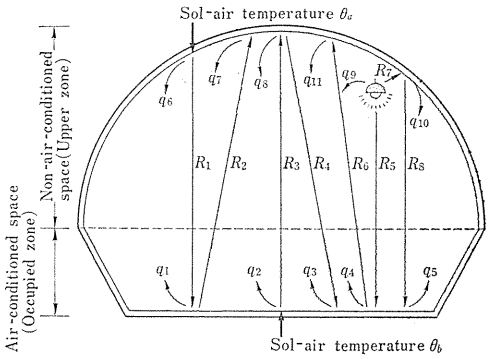

Fig. 48. Illustration of cooling load elements in the occupied zone.

Sensible heat extraction from the air-conditioned occupied zone at the time n is expressed as follows.

$$q_{r,n}=\sum_{k=1}^{6} q_k+c_p\cdot\gamma\cdot V\overline{K}(\theta_{u,n}-\theta_{r,n}) \tag{11}$$

The equation of heat balance in the non air-conditioned upper zone is expressed as follows:

Table 6. List of the symbols.

Symbols	
θ_a, θ_b	sol-air temperature
θ_u, θ_r	average temperature in the upper zone and in the occupied zone respectively
α_f, α_{fc}, α_{fr}	total, convective, radiant heat transfer coefficient on the wall surfaces in the occupied zone
α_i, α_{ic}, α_{ir}	total, convective, radiant heat transfer coefficient on the wall surfaces in the upper zone
Y, Z	response factors of the wall surfaces in the upper zone
Y', Z'	response factors of the wall surfaces in the occupied zone
$WG_{i,j}$, $WG_{f,j}$	weighting factors of wall surfaces in the upper zone and in the occupied zone relating space cooling loads to radiant heat
L_n	the amounts of inner heat generation (Kcal/h)
k, k'	the rate of convection, upward radiation of L_n
A_i, A_f	wall areas of upper zone, occupied zone respectively
c_p, γ	constant-pressure specific heat, specific weight of room air
$\overline{K}$	imaginary ventilation rate between the upper zone and the occupied zone
V	volume of the upper zone (m^3)

$$\sum_{k=6}^{11} q_k = c_p \cdot \gamma \cdot V \cdot \frac{d\theta_u}{dt} + c_p \cdot \gamma \cdot V \cdot \overline{K}(\theta_{u,n} - \theta_{r,n}) \tag{12}$$

where

$$q_1 = (\alpha_{fc}/\alpha_f) \times \left(\sum_{j=0}^{\infty} WG_{f,\,j} \times R_{1,\,n-j}\right)$$

$$q_2 = (\alpha_{fc}/\alpha_f) \times \left(\sum_{j=0}^{\infty} Y'_j \cdot \theta_{b,\,n-j} - \sum_{j=0}^{\infty} Z'_j \times \theta_{r,\,n-j}\right) \times A_f$$

$$q_3 = \sum_{j=0}^{\infty} WG_{f,\,j} \times R_{4,\,n-j}$$

$$q_4 = (\alpha_{fc}/\alpha_f) \times \left(\sum_{j=0}^{\infty} WG_{f,\,j} \times R_{5,\,n-j}\right)$$

$$q_5 = \sum_{j=0}^{\infty} WG_{f,\,j} \times R_{8,\,n-j}$$

$$q_6 = (\alpha_{ic}/\alpha_i) \times \left(\sum_{j=0}^{\infty} Y_j \cdot \theta_{a,\,n-j} - \sum_{j=0}^{\infty} Z_j \cdot \theta_{u,\,n-j}\right) \times A_i$$

$$q_7 = \sum_{j=0}^{\infty} WG_{i,\,j} \times R_{2,\,n-j}$$

$$q_8 = (\alpha_{ic}/\alpha_i) \times \left(\sum_{j=0}^{\infty} WG_{i,\,j} \times R_{3,\,n-j}\right)$$

$$q_9 = k \times L_n$$

$$q_{10}=(\alpha_{ic}/\alpha_i)\times(\sum_{j=0}^{\infty} WG_{i,\,j}\times R_{7,\,n-j})$$

$$q_{11}=\sum_{j=0}^{\infty} WG_{i,\,j}\times R_{6,\,n-j}$$

$$R_1=(\alpha_{ir}/\alpha_{ic})\times q_6 \qquad R_2=(\alpha_{fr}/\alpha_{fc})\times q_1$$

$$R_3=(\alpha_{fr}/\alpha_{fc})\times q_2 \qquad R_4=(\alpha_{ir}/\alpha_{ic})\times q_8$$

$$R_5=(1-k-k')\times L_n \qquad R_6=(\alpha_{fr}/\alpha_{fc})\times q_4$$

$$R_7=k'\times L_n \qquad R_8=(\alpha_{ir}/\alpha_{ic})\times q_{10}$$

$$\begin{cases} WG_{i,\,0}=1-Z_0/\alpha_i & (j=0) \\ WG_{i,\,j}=-Z_j/\alpha_i & (j\geqq 1) \end{cases} \qquad \begin{cases} WG_{f,\,0}=1-Z'_0/\alpha_f & (j=0) \\ WG_{f,\,j}=-Z'_j/\alpha_f & (j\geqq 1) \end{cases}$$

We can get the unknown $\theta_{u,n}$, $q_{r,n}$ by solviog the eq. (11) and (12) as simultaneous equations. In this calculation the value of $\overline{K}$ must be given and can be obtained from the model experiments. Recommended values of $\overline{K}$ are shown in Table 7.

Table 7, Recommendation value of $\overline{K}$,

Installed height of outlets from floor		$\overline{K}$
in the middle of walls	with ventilation system in the upper zone	6.0
	without ventilation system in the upper zone	8.0
near the floor surfaces	with ventilation system in the upper zone	4.0
	without ventilation system in the upper zone	6.0

7. 2. Comparison of Heat Load between the Calculated and the Actually Measured in the M-Factory

Measurements of cooling load in the M-Factory which is described in Chapter 6 of this paper were performed in August, 1973 in order to examine the accuracy of proposed calculation method. The solar incidence, outside air temperature and room air temperature were measured at the same time.

Fig. 49 shows the results of the comparison on the heat extraction rate between the actually measured and the calculated by using the proposed method under summer cooling conditions. The heat extraction rate in the actual building

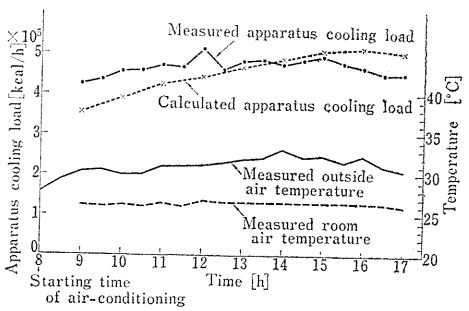

Fig. 49. Comparison of measured apparatus cooling load with the calculated cooling load. (August, 20, 1973)

was estimated as the total heat by measuring the temperature difference of chilled water between supply and return, and the water flow rate. On the other hand, the calculation of heat extraction rate was carried out hour by hour with the measured values of internal and external conditions. The $\overline{K}$ value was assumed to be 6.0 in this calculation.

The rate of latent heat transfer from the upper zone to the occupied zone by imaginary air change was not taken into account, because the value of $\overline{K}$ for latent heat transfer was unknown. Therefore, the calculated value should be increased by about 10~20% for compensation. Considering the fact as described above, the measured and calculated cooling loads are recognized to be nearly equal, which assures considerable reliability of the proposed calculation method.

7. 3. Examination of Economical Feasibility for the Occupied Zone Air-Conditioning

Fig. 50 and Table 8 give the basis of economical feasibility for the occupied zone air-conditioning as compared with the conventional (whole space) air-conditioning of the building. It is understood that the cooling load with the occupied zone air-conditioning can be reduced to almost half of the load with the conventional and contributes to the reduction of the initial and operating costs of the air-conditioning system.

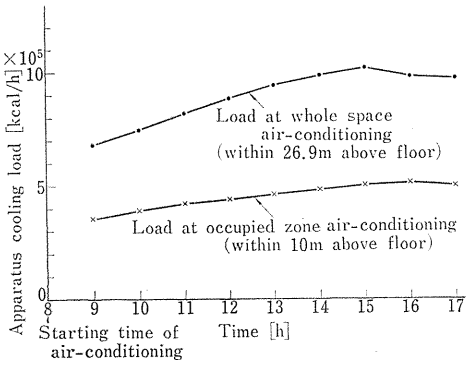

Fig. 50. Comparison of apparatus cooling load between the occupied zone air-conditioning and the whole space air-conditioning. (calculated values)

Table 8. Comparison of cooling loads in two types of air-conditioning system.

Various Cooling Loads	Occupied Zone Air-Conditioning	Whole Space Air-Conditioning
Load from Roof	10,300	109,700
Load from Walls	37,000	113,500
Load from Machines	266,000	266,000
Load from Light	13,700	93,100
Load from Air-Conditioner	38,300	61,000
Load from Persons	6,800	6,800
Load from Crane		188,300
Outside Air Load	88,500	88,500
Heat Loss from Pipes and Ducts	46,100	92,700
Total Cooling Load (Apparatus Cooling Load)	506,700	1,019,600

8. Conclusion

1) In the scaled model experiments of the air distribution within a turbulent room, it was recognized that the temperature distribution with fair degree of reliability could be obtained only from the similarity theory to have the Archimedes numbers both for the model and the actual matched. It was also found that the experiments by using the partial model based on the symmetry of buildings were effective in enlarging the scale of models to assure more accuracy of the experiments.

With regard to the similarity of air velocity distribution in the model tests, the degree of accuracy could not be examined sufficiently because of the difficulty of actual measurements and the unreliability of anemometer in the range of low air velocity. Considering the close relation between velocity distribution and temperature distribution in the room, however, a good agreement of air velocity between the model and the actual is supposed to have been established.

2) It was proved that the cooling load for large spaces could be reduced remarkably in the case of the occupied zone air-conditioning as compared with the conventional air-conditioning to cover whole space, and that the proposed system contributes to economy and energy conservation, though needless to say, the reduction rate of heat load depends upon the shape, use, thermal characteristics and amounts of the inside heat generation of buildings.

3) Among the variations of the occupied zone air-conditioning system for large spaces, an optimum system must be selected according to various characteristics of the building. In any case, the separation of air-conditioning system for the occupied zone from ventilation system for the upper zone is fairly effective in removing heat, dust and smoke stagnant in the upper zone, because considerably lower temperature of recirculated exhaust air or outside air than that of the roof is applied for the upper zone ventilation.

4) In the air-conditioning for large spaces more uniform distribution of air temperature and velocity in the occupied zone can be obtained if the proper arrangement of air outlets and inlets is made, and if proper shapes of outlets, such as the induction type, which acceleralate air flow near the outlets and increase the effective air change rate are adopted.

5) It was recognized that the proposed calculation method of cooling load for the occupied zone air-conditioning in large spaces was fairly accurate and practical, enabling the prediction of the degree of economy and energy savings.

Acknowledgements

The author acknowledges the original advice for the study by the late professor of Tokyo University, Dr. G. Nomura, and also gives great thanks to Mr. T. Goto, Mr. Y. Miyakawa, Mr. M. Kobayashi, Mr. T. Yasuda and Mr. S. Ito, who belong to Ohbayashi-gumi Ltd., for the cooperation in practicing those experiments and actual measurements as well as design of air-conditioning systems of those buildings.

Reference

1) Nakahara, Goto and Miyakawa: Experiments with Scale Models and Actual Measurement on Space Air Distribution, -Part 1, Transactions of SHASE Japan Vol. 11, 1973.
2) Kobayashi, Yasuda, Ito and Miyakawa: Experiments with Scale Models and Actual Measurement on Space Air Distribution, -Part 2, Transactions of SHASE Japan Vol. 13, 1975.
3) Y. Miyakawa: A Calculation Method of Heat Loads for Limited Occupied Zone Air-Conditioning of Larger Hall, Collective Abstracts, Academic Research Symposium, Architectural Institute of Japan 1974, 10.
4) B. Gebhart: A New Method for Calculating Radiant Exchanges, ASHRAE Transactions, Vol. 65, 1959.
5) Baturin: Lüftungsanlagen für Industriebauten.
6) Shoda and Tsuchiya: Methods of Experiments with Scale Models on Air Distributions in Rooms, 38th Collective Abstracts, Kanto Chapter, Architectural Institute of Japan, 1967.
7) Maeda, Ishiguro and Matsumoto: Similarity Theory for Heat Convection in a Room, Collective Abstracts, Academic Research Symposium, Architectural Institute of Japan, 1959, 10.
8) Tsuchiya, Shoda and Terasawa: Experimental Study on Coefficient of Vortex Viscosity in a Room, Collective Abstracts, Academic Research Symposium, Architectural Institute of Japan, 1969.
9) Ibamoto: A Combined Theory of Model Experiments in a Heating Room, Collective Abstracts, Academic Research Symposium, Architectural Institute of Japan, 1960.
10) B. Regenscheit: Die Archimedes Zahl, Kennzahl zur Beurteilung von Raumströmungen, Gesundheits-Ingenieur, Heft 6, 1970.
11) H. Brockmeyer: Die Strahllüftung der Olympia-Sport-Halle, Untersuchung am Model und an der Anlage, Gesundheits-Ingenieur, Heft 6, 1972.
12) Henry L. Langhaar: Dimentional Analysis and Theory of Models